Vacuum 143 (2017) 138–149

Contents lists available at ScienceDirect

Vacuum

journal homepage: www.elsevier.com/locate/vacuum

Effective atomic number and buildup factor calculations for metal nano particle doped polymer gel

P. Sathiyaraj [a, *], E.J.J. Samuel [a], C.C.S. Valeriano [b], M. Kurudirek [c]

[a] Medical Gel Dosimeter Laboratory, Department of Physics, VIT-University, Vellore 632014, Tamil Nadu, India
[b] Institute of Pesquisas Energeticas e Nucleares, Cidade Universitaris, Av. Prof. Lineu prestes, 2242 Sao Paulo, Brazil
[c] Department of Physics, Faculty of Science, Ataturk University, 25240 Erzurum, Turkey

ARTICLE INFO

Article history:
Received 18 January 2017
Received in revised form
17 March 2017
Accepted 4 June 2017
Available online 6 June 2017

Keywords:
PAGAT
Effective atomic number
XCOM
Buildup factor
Mass attenuation coefficient

ABSTRACT

The present study aimed at verifying the water equivalency of the PAGAT gel and metal nano particle (different concentration of gold and silver) PAGAT (MPAGAT) gel in terms of effective atomic number (Z_{eff}). In addition to Z_{eff}, energy absorption buildup factor (EABF) and exposure buildup factor (EBF) have been calculated for MPAGAT. Auto-Z_{eff} computer program was used to calculate the effective atomic number for MPAGAT in the energy region 10 keV to 1 GeV. EABF and EBF were calculated by using geometric progression (GP) fitting formula in the energy region from 0.015 to 15 MeV up to penetration depths of 40 mean free path. Mass attenuation coefficient of MPAGAT gel was obtained by the XCOM program and the results were compared with Monte Carlo simulation. It has been found that Au and Ag doped PAGAT gels show excellent water equivalency than undoped PAGAT gel at dopant concentrations of 0.1, 0.5 and 1 mM. From the results, it was noted that the EABF and EBF were significantly varied with respect to photon energy and chemical composition of given PAGAT gel with different concentration of metal nano particle. Since mass attenuation coefficients were used to obtain Z_{eff} and EABF, the reliability of the mass attenuation coefficient data were cross checked with Monte Carlo simulation, and a good agreement was obtained between XCOM and Monte Carlo simulation.

1. Introduction

Verification of complex three dimensional radiation dose distributions is an important process in advanced radiotherapy modalities such as IMRT, IGRT and SRS/SRT [1]. Due to a lot of dose gradients in dose distribution, it is necessary to use dosimeters with high spatial resolution to estimate dose accurately. Polymer gels are promising 3d dosimeters with high spatial resolution in addition to its superior radiological and dosimetric properties such as water and/or tissue equivalency, energy and dose rate independency, angular independency [2]. They act as detector and phantom, thus perturbation correction factors are not necessarily needed. These advantages of polymer gels make a huge footprint in the field of medical physics. Developments in this field are being directed in different aspects of polymer gels production such as increasing melting point [3], increasing sensitivity [4] and testing dose enhancement effect (DEE) by metal nano particles (MNP) [5,6]. In order to evaluate the DEE in gel, different MNPs were used by many researchers and they successfully reported the DEE in polymer gels [6]. Since water or tissue equivalency of the polymer gel depends on the elemental composition, atomic numbers of elements and incident photon energy it would be useful to check the radiological properties of polymer gel in parallel of DEE research.

In the present study, an attempt has been made to check how MNPs doped polymer gel differs in terms of its Z_{eff} and EABF and EBF. Literature is rich of studies related to the computing Z_{eff} and buildup factor [7–15]. Since, Z_{eff} depends on the photon beam energy; defining Z_{eff} of a particular compound by a single value is not the appropriate way [7]. Therefore, it would be useful to verify the Z_{eff} in a continuous range of energy. Z_{eff} is very useful in choosing a substitute composite material in place of an element for a specific energy depending on the requirement. Once photon enters into the medium it degrades its energy and dose buildup occurs inside the medium. The dose deposition in the medium depends on intensity of incident beam. The attenuation of intensity of the incident beam obeys the well-known Lamberts Beer's law if the beam is mono energetic, narrow and interacts with thin absorbing medium. In case if any of the above conditions is not met, the

* Corresponding author.
E-mail address: sathiarajmedphy@gmail.com (P. Sathiyaraj).

http://dx.doi.org/10.1016/j.vacuum.2017.06.005
0042-207X/

Lamberts Beer's law can be applied by incorporating multiplicative correction factor, called the "Buildup factor". Then we have to use the modified Lamberts Beer law ($I = \mathbf{BI_0e^{-\mu x}}$) where B is the buildup factor. Presence of inorganic materials i.e. dopants can make the gel greatly vary with respect to their Z_{eff} and EABF. Many of the radiological properties of the gel were reported in literature [16–18]. However, the effect of metal doping in the gel has not been investigated yet in terms of buildup factor and effective atomic number. This motivated us to carry out this work.

2. Method of computation

Firstly Z_{eff} for the PAGAT was calculated using Mayneourd's formula [19] for different concentration of Au and Ag in the gel as:

$$Z_{eff} = \left(a_1 Z_1^{2.94} + a_2 Z_2^{2.94} + \ldots a_i Z_i^{2.94}\right)^{1/2.94} \quad (1)$$

where a_1, a_2, a_3,… a_i, are the fractional contributions of each element to the total number of electrons in the gel. Z is the atomic number of each element present in the gel. Tables 1 and 2 shows the fractional contribution of each element in the gel. Table 3 shows the Z_{eff} of Au and Ag doped PAGAT gel dosimeter.

2.1. Effective atomic number

Auto-Zeff program is a user-friendly software in visual basic base for rapid computation of the effective atomic numbers and spectral-weighted mean atomic numbers. In this method, effective atomic number is determined via exploitation of the smooth correlation between atomic cross-section and atomic number. A matrix of cross-sections was constructed spanning atomic number for photon energies ranging between 10 keV and 1 GeV and the cross-sections of poly-elemental media are calculated by linear additivity rule. The cross-sectional values are constructed with the cross-section matrix as a function of Z, and an effective atomic number is obtained by the interpolation of Z values between adjacent cross-section data [20].

Table 1
Elemental composition of Au doped MPAGAT.

Elements	Fraction of weight (Au doped PAGAT gel)				
	0.1 mM	1 mM	5 mM	10 mM	100 mM
H	0.107255	0.107236	0.107046	0.105185	0.106548
C	0.062173	0.062162	0.062052	0.060973	0.061763
N	0.019688	0.019684	0.019649	0.019308	0.019558
O	0.80215	0.802008	0.800589	0.786671	0.803474
P	0.004064	0.004063	0.004056	0.003985	0.004037
Cl	0.004651	0.00465	0.004642	0.004561	0.00462
Au	0.00002	0.000197	0.001966	0.019316	0.106548

Table 2
Elemental composition of Ag doped MPAGAT.

Elements	Fraction of weight (Ag doped PAGAT gel)				
	0.1 mM	1 mM	5 mM	10 mM	100 mM
H	0.107256	0.107245	0.107199	0.107141	0.106112
C	0.062173	0.062167	0.06214	0.062107	0.06151
N	0.019688	0.019686	0.019677	0.019667	0.019478
O	0.802157	0.802079	0.801734	0.801302	0.793606
P	0.004064	0.004064	0.004062	0.00406	0.004021
Cl	0.004651	0.00465	0.004648	0.004646	0.004601
Ag	0.000011	0.000108	0.000539	0.001078	0.010672

Table 3
Effective atomic number of Au and Ag doped PAGAT gel.

Concentration (mM)	Z_{eff} for Au doped PAGAT	Z_{eff} for Ag doped PAGAT
0.1	7.798116	7.755646
1	8.201845	7.806176
5	9.650657	8.023406
10	11.01288	8.279979
100	21.01493	11.41948

2.2. Buildup factor

BF depends on the amount of scattering which in turn depends on the photon energy and the nature of the medium. In addition the build-up factor will depend on the distance of the dose point from the source measured in mean free paths. The buildup factors can be classified in to two types: 1. Energy absorption buildup factor (EABF) that is the buildup factor in which the quantity of interest is the absorbed energy of the photons in the medium and 2. Exposure buildup factor (EBF) that is the buildup factor in which the quantity of interest is the exposure in the air after penetrating through the absorber [21].

American National Standards ANSI/ANS-6.4.3 published the BF data for 23 elements (Z = 4 to 92) and it covers the photon energy from 0.015 to 15 MeV for 40 mean free path (mfp) and is obtained by geometric fitting progression method (GP) [22]. The logarithmic interpolation method was used to calculate the buildup factor co-efficients using GP fitting parameters from respective equivalent atomic numbers (Z_{eq}) of the target materials. The following steps were involved in computing BF: 1. Calculation of the Z_{eq}, 2. Calculation of GP fitting parameters, and 3. Calculation of buildup factor. Z_{eq} is similar to atomic number of given compound and it is varying with respect to different energy. Total interaction of photons with materials is composed of different partial interactions such as photoelectric absorption, Compton scattering and pair production. In both photoelectric and pair production processes, photons are completely absorbed but, in Compton process many scattered radiation came out and it therefore contributes significantly in buildup of photons.

2.2.1. Computation of Z_{eq} and G.P fitting parameter for EABF and EBF calculation

Z_{eq} was computed for plain PAGAT (P.PAGAT) and metal doped PAGAT (MPAGAT) for different concentration of Au and Ag. Ratio of total interaction to Compton scattering was considered for calculating Z_{eq} since BF mainly arises from Compton scattering.

To calculate Z_{eq}, first Compton mass attenuation coefficient ($(\mu/\rho)_{Comp}$) and total mass attenuation co-efficient ($(\mu/\rho)_{total}$) were obtained for the pure elements, P.PAGAT and MPAGAT using XCOM [23] data base.

The equivalent atomic number, Z_{eq}, for P.PAGAT and MPGAT was then calculated by matching the $(\mu/\rho)_{Comp}/(\mu/\rho)_{total}$, of the given gel dosimeter at a given energy with the corresponding ratio of a pure element at the same energy. If this ratio lies between the two ratios for known elements, then the value of Z_{eq} is interpolated using the following logarithmic interpolation formula [24]:

$$Zeq = \frac{Z_1(\log R_2 - \log R) + Z_2(\log R - \log R_1)}{(\log R_2 - \log R_1)} \quad (2)$$

where Z_1 and Z_2 are the atomic numbers of two adjacent elements, R_1 and R_2 are the ratios $(\mu/\rho)Comp/(\mu/\rho)total$ for these elements, and R is the corresponding ratio for P.PAGAT and MPAGAT at a given energy, which lies between R_1 and R_2 (adjacent to R). Tables 1 and 2 shows the Z_{eq} of Au and Ag doped MPAGAT and P.PAGAT gel.

In order to calculate the G.P fitting parameter the same above

mentioned interpolation method was followed. The GP fitting parameters for elements were taken from the ANSI/ANS-6.4.3 standard reference database which provides the GP fitting parameters for twenty three elements (Be, B, C, N, O, Na, Mg, Al, Si, P, S, Ar, K, Ca, Fe, Cu, Mo, Sn, La, Gd, W, Pb and U) in the energy region 0.015–15 MeV up to 40 mfp. The GP fitting buildup factor coefficients of the gel can be calculated by the following equation

$$C = \frac{C_1\left(\log Z_2 - \log Z_{eq}\right) + C_2\left(\log Z_{eq} - \log Z_1\right)}{\left(\log Z_2 - \log Z_1\right)} \quad (3)$$

where C_1 and C_2 are the values of the coefficients (GP fitting parameters) corresponding to the atomic numbers of Z_1 and Z_2, respectively, and Z_{eq} is the equivalent atomic number of the given material.

Final step is calculation of buildup factor using the GP fitting parameters.

$$B(E,X) = 1 + \frac{b-1}{(K-1)}\left(K^x - 1\right) \quad \text{for } K \neq 1$$

$$B(E,X) = 1 + (b-1)x \quad \text{for } K = 1$$

$$K(E,X) = cx^a + d\frac{\tanh\left(x/X_k - 2\right) - \tanh(-2)}{(\tanh - 2)} \quad \text{for } x \leq 40\text{mfp}$$

where x is the penetration depth in mfp (the average distance traveled by a photon between successive interactions), and b, the value of the energy absorption buildup factor at 1 mfp, K (E, x), K is the photon dose multiplication factor and change in the shape of spectrum with increasing penetration depth, x. K is represented by tangent hyperbolic function of penetration depth in mfp. And b, c, a, X_K and d are computed G-P fitting parameters which depends on the attenuating medium and source energy.

2.3. Monte Carlo calculation of mass attenuation coefficients

The MCNP5-1.60 was used to simulate the PAGAT's irradiation. In a random way three concentrations were chosen for the simulation of the PAGAT: the first one was the PLAIN PAGAT (without nanoparticle); the gel with 1 mM of Au nanoparticle; and the gel with 1 mM of Ag. Similarly, three photon energies were chosen for each concentration. For each scenario, a conical shaped radioactive source with a radii of 36 mm was used. A system of three cylindrical collimators of lead was used; each one consists of 10 mm thickness. Once the concentration of nanoparticle and the energy were fixed, the plates were positioned in order to represent the gel. These plates have 100 mm of width and length. A lot of archives were created, each with a different length, in order to analyze the difference of attenuation for different thicknesses. First, a scenario without a gel plate was simulated, representing the intensity without attenuation (I_0). Thereafter, the simulation was made for a variety of thickness of the plates in order to represent the intensity variation (I). For simulation of the response of the detector i.e. an ionization chamber, PTW 23344) it was used the tally of energy deposition, tally F6 in MeV/g [25], at the sensible volume of the ionization chamber. For all scenarios, 9E08 histories were used. Fig. 1 shows the simulation geometry.

3. Results and discussion

Table 3 shows the Z_{eff} of MPAGAT using Mayneourd's formula

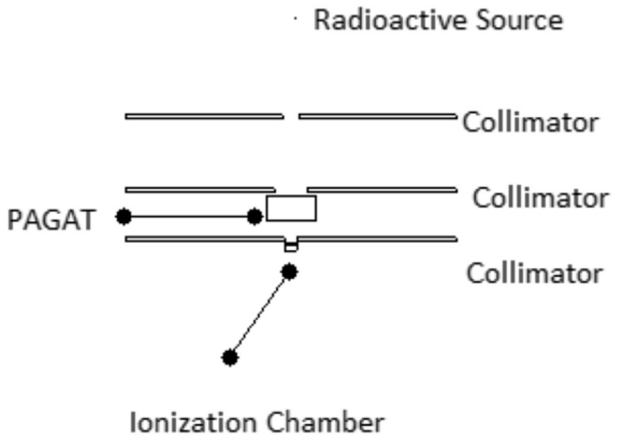

Fig. 1. Monte Carlo simulation geometry for irradiation of PAGAT with ion chamber.

[19]. The values of Z_{eff} increased as the concentration of heavy elements increase in the gel dosimeter. In this calculation method, Z_{eff} is given as a function of elemental composition of the gel only and only a single value can be obtained for the given material irregardless of changing photon energy. Since, the Au has higher atomic number than Ag, its respective Z_{eff} is higher than Ag. However, it should be noted that partial photon interaction processes, thus mass attenuation coefficients have photon energy dependence in a continuous energy region. Therefore, a method in which energy dependence is taken into account would be more convenient to calculate Z_{eff}. The energy dependent Z_{eff} will be discussed in detail in the following sections.

3.1. Effective atomic number of Au doped MPAGAT

Variations in Z_{eff} of PAGAT (without Au), MPAGAT (with different concentration of Au) with respect to energy are shown in Fig. 2. All Z_{eff}s initially increase with energy from 0.01 MeV to 0.02 MeV due to dominant process of photoelectric absorption but, higher values of Z_{eff} were obtained at 50 and 100 mM concentration due to more abundance of Au than other concentration and, therefore this might increase the interaction cross section for photoelectric absorption process. Beyond 0.02 MeV the rapid fall occurs up to 0.1 MeV in the

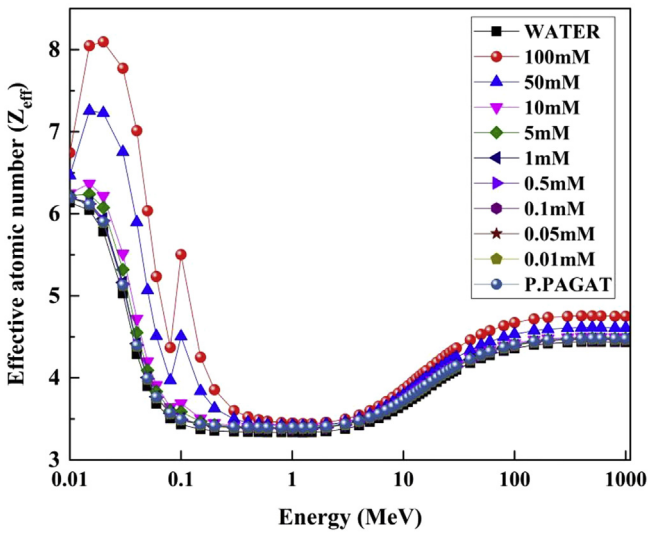

Fig. 2. Effective atomic number of Au doped MPAGAT for different concentration.

concentration range of 0.01 mM–10 mM. In higher concentration (50 and 100 Mm) the rapid fall extends up to 0.3 MeV. Since Compton cross section is proportional to Z, the variation of Z_{eff} was constant from 0.4 to 2 MeV. Beyond 2 MeV, pair production takes over the Compton scattering and Z_{eff} gradually increases up to 200 MeV. It should be noted that at around 100 keV which is very close to the K-absorption edge of Au i.e. 81 keV there appears to be a sudden increase in values of Z_{eff} (Fig. 2). This is due to the fact that two possible mass attenuation coefficients, thus Z_{eff}s can be obtained one corresponding to the lower side and the other to the upper side of the same energy, which leads a non-uniform variation of Z_{eff} at around absorption edges.

The relative deviation (%RD) of Au doped M.PAGAT from water was calculated and shown in Fig. 3. From 0.01 to 0.2 MeV %RD was greater than 6% in 10 mM doped MPAGAT and maximum %RD was 10% at this energy region. Above 0.2 MeV the % RD was less than 1.6%.

For 5 mM doped MPAGAT the % RD is greater than 4% from 0.01 to 0.15 MeV and maximum deviation was 6.14%. Above 0.15 MeV it was less than 1.4%. From 0.01 mM to 10 mM all Au doped MPAGATs differ from water with a relative difference of 2.7% for the energy range of 10 keV to 1 GeV. Reduction in the %RD for higher energy might be due to the lower photoelectric interaction cross section in these energies.

In higher concentration (50 and 100 mM) the average % RD thru the entire energy region were 6% and 12% for 50 and 100 mM, respectively. In higher concentration of Au, photoelectric cross section is higher than that of lower concentration due to production of more secondary radiation and they might have enough energy to knock out the K or L shell electron of Au. From 0.01 mM to 1 mM concentration, doped MPAGAT seems to be better water equivalent than P.PAGAT (Relative differences are 1.51%, 1.32%, 1.3%, 1.21%, 1.20% and 1.22% for P.PAGAT, 1 mM, 0.5 mM, 0.1 mM, 0.05 mM, 0.01 mM doped MPAGAT respectively). Except for 50 and 100 mM, gels with all other concentrations did not show much discrepancy in terms of water equivalent property.

3.2. Effective atomic number of Ag doped MPAGAT

Ag doped M.PAGAT holds the same argument of Au doped M.PAGAT. Variations in Z_{eff} of PAGAT (without Ag), MPAGAT (with different concentration of Au) and water with respect to energy are shown in Fig. 4. Z_{eff} of gels doped from 0.01 to 10 Mm was higher at

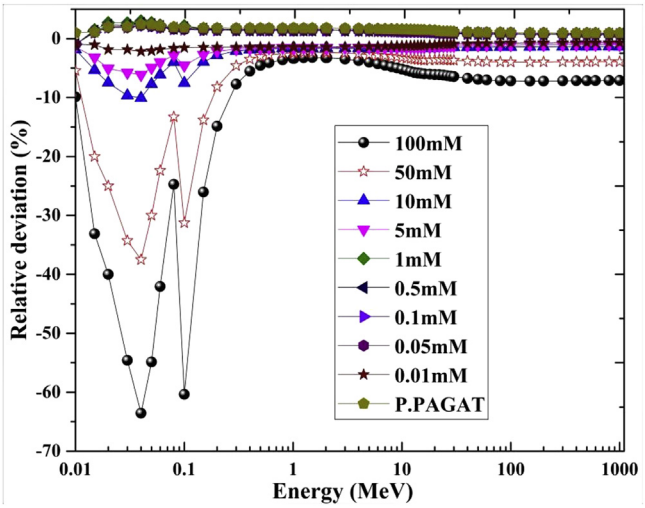

Fig. 3. Relative deviation in Z_{eff} of Au doped MPAGAT with respect to water.

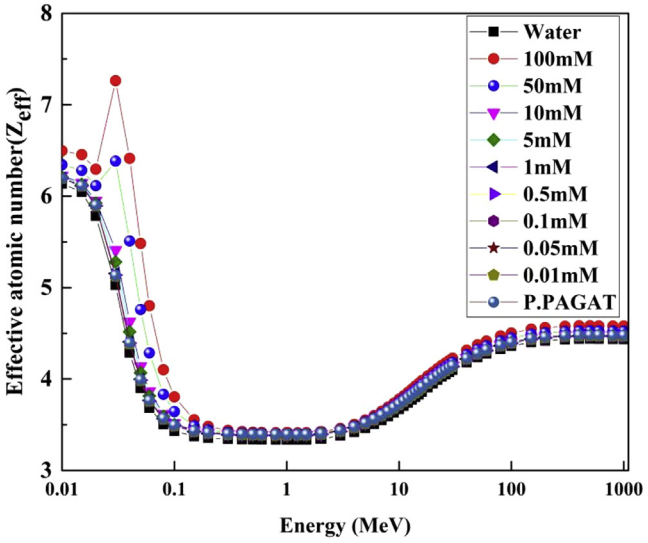

Fig. 4. Effective atomic number of Ag doped MPAGAT for different concentration.

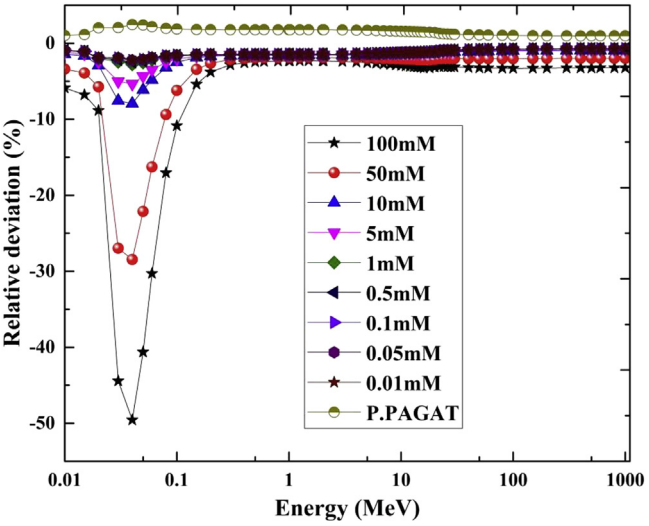

Fig. 5. Relative deviation in Z_{eff} of Ag doped MPAGAT with respect to water.

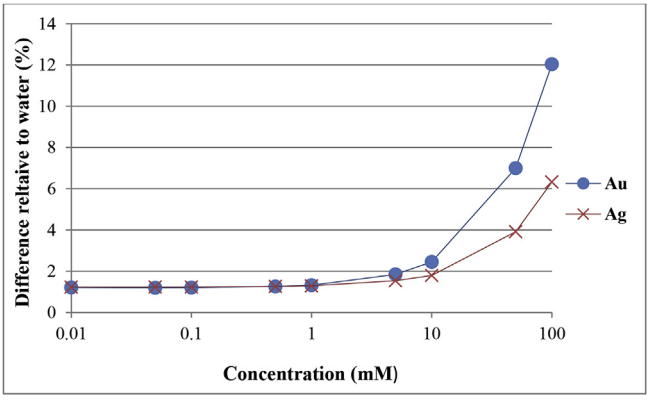

Fig. 6. Relative deviation % in effective atomic number relative to water as function of Au and Ag concentration.

initial energy i.e. 0.01 MeV due to photoelectric absorption, after that the rapid fall was noticed up to 0.15 MeV. For 50 and 100 mM doped gel dosimeters, the maximum Z_{eff} was found at K-edge of Ag and start decreasing beyond the K-edge up to 0.15 MeV. K-edge influence was significant at higher concentrations (50 and 100 Mm) and it is not much affected for the rest of the concentrations. From 0.3 to 2 MeV Z_{eff} for all concentrations were constant. Beyond 2 MeV, it started gradually increasing up to 150 MeV due to pair-production. After 150 MeV the constant pattern was observed for Z_{eff} for all the concentrations.

The RD% in Z_{eff} of Au doped M.PAGAT with respect to water was calculated and is shown in Fig. 5. For 100 mM concentration, over all RD% was 6.3% and maximum value was 49.6%. For 50 Mm concentration over all RD% was above 4%. From 0.01 to 0.3 MeV it was greater than 11%, beyond 0.3 MeV it was less than 2.1%. For 10 mM concentration, the RD% was greater than 4.2% from 0.01 to 0.15 MeV, beyond 0.15 MeV it was less than 1.4%. For 5 mM, the maximum RD% was 3.2% from 0.01 to 0.08 MeV. Beyond 0.08 MeV it was less than 1.3%. For the concentration range of 0.01 mM−10 mM, the RD% was less than 1.8% in the energy range from 10 keV to 1 GeV. From 0.01 mM to 1 mM, doped MPAGAT has shown less difference when compared to water than P.PAGAT (1.51%, 1.29%, 1.26%, 1.24%, 1.23% and 1.23% for P.PAGAT, 1 mM, 0.5 mM, 0.1 mM, 0.05 mM, 0.01 mM doped MPAGAT, respectively).

Table 4
Equivalent atomic number of P.PAGAT and Au doped MPAGAT.

Energy (MeV)	P.PAGAT	0.1 mM	0.5 mM	1 mM	5 mM	10 mM	50 mM	100 mM
0.015	7.36	7.36	7.38	7.4	7.59	7.8	9.23	10.37
0.02	7.38	7.39	7.41	7.44	7.66	7.91	9.51	10.77
0.03	7.4	7.41	7.44	7.48	7.75	8.06	9.91	11.32
0.04	7.41	7.42	7.45	7.49	7.82	8.17	10.21	11.72
0.05	7.42	7.42	7.46	7.51	7.88	8.26	10.44	12.03
0.06	7.42	7.43	7.47	7.52	7.94	8.33	10.63	12.29
0.08	7.42	7.44	7.49	7.55	8.02	8.46	10.97	12.69
0.1	7.43	7.5	7.77	8.09	9.78	11.16	16.4	20.7
0.15	7.44	7.53	7.88	8.23	10.22	11.75	17.39	20.9
0.2	7.44	7.54	7.96	8.34	10.5	12.14	18.03	21.64
0.3	7.44	7.57	8.05	8.5	10.92	12.64	18.82	22.57
0.4	7.45	7.59	8.1	8.6	11.15	12.98	19.3	23.15
0.5	7.45	7.6	8.14	8.68	11.3	13.17	19.62	23.52
0.6	7.45	7.61	8.17	8.73	11.41	13.3	19.84	23.77
0.8	7.45	7.62	8.2	8.78	11.52	13.43	20.06	24.03
1	7.45	7.62	8.2	8.8	11.55	13.47	20.13	24.11
1.5	6.59	6.6	6.64	6.7	7.15	7.71	11.86	15.94
2	6.54	6.55	6.56	6.57	6.7	6.85	8.13	9.63
3	6.53	6.54	6.54	6.55	6.61	6.69	7.34	8.08
4	6.53	6.53	6.53	6.54	6.59	6.65	7.19	7.78
5	6.53	6.53	6.53	6.54	6.58	6.64	7.12	7.66
6	6.52	6.53	6.53	6.53	6.58	6.63	7.09	7.59
8	6.52	6.52	6.52	6.53	6.57	6.62	7.05	7.52
10	6.52	6.52	6.52	6.53	6.56	6.61	7.03	7.49
15	6.51	6.52	6.52	6.52	6.56	6.60	7.00	7.45

Table 5
Equivalent atomic number of P.PAGAT and Ag doped MPAGAT.

Energy (MeV)	P.PAGAT	0.1 mM	0.5 mM	1 Mm	5 mM	10 mM	50 mM	100 mM
0.015	7.36	7.36	7.36	7.36	7.39	7.39	7.78	8.03
0.02	7.38	7.39	7.39	7.39	7.42	7.42	7.85	8.13
0.03	7.4	7.41	7.43	7.46	7.67	7.67	9.47	10.69
0.04	7.41	7.42	7.44	7.47	7.72	7.72	9.74	11.07
0.05	7.42	7.42	7.45	7.49	7.77	7.77	9.95	11.37
0.06	7.42	7.43	7.46	7.5	7.81	7.81	10.1	11.54
0.08	7.42	7.43	7.47	7.51	7.87	7.87	10.32	11.86
0.1	7.43	7.44	7.48	7.53	7.92	7.92	10.49	12.09
0.15	7.44	7.45	7.49	7.55	8	8	10.79	12.44
0.2	7.44	7.45	7.5	7.56	8.04	8.04	10.99	12.68
0.3	7.44	7.46	7.51	7.58	8.1	8.1	11.19	12.99
0.4	7.45	7.46	7.52	7.59	8.13	8.13	11.31	13.14
0.5	7.45	7.46	7.52	7.6	8.15	8.15	11.39	13.23
0.6	7.45	7.46	7.53	7.61	8.16	8.16	11.44	13.29
0.8	7.45	7.46	7.53	7.61	8.18	8.18	11.49	13.35
1	7.45	7.46	7.53	7.61	8.18	8.18	11.5	13.36
1.5	6.59	6.59	6.59	6.6	6.65	6.65	7.32	7.98
2	6.54	6.54	6.55	6.55	6.57	6.57	6.88	7.15
3	6.53	6.53	6.54	6.54	6.55	6.55	6.79	6.99
4	6.53	6.53	6.53	6.53	6.55	6.55	6.76	6.94
5	6.53	6.53	6.53	6.53	6.54	6.54	6.75	6.93
6	6.52	6.53	6.53	6.53	6.54	6.54	6.75	6.91
8	6.52	6.52	6.52	6.52	6.54	6.54	6.74	6.9
10	6.52	6.52	6.52	6.52	6.53	6.53	6.73	6.89
15	6.51	6.51	6.52	6.52	6.53	6.53	6.73	6.88

When the concentration of MNP increased beyond 1 mM the discrepancies in Z_{eff} of MPAGAT increased with the increase in dopant concentration (Fig. 6).

3.3. Build up factor

The energy absorption buildup factor (EABF) was calculated for all the concentration of gel from 0.5 to 40mfp. Tables 4 and 5 shows the calculated Z_{eq} of Au and Ag doped MPAGAT and P.PAGAT gel.

3.4. Variation of energy absorption buildup factor with energy for Au and Ag doped MPGAT

Figs. 7 and 8 show graphical representation of EABF for P.PAGAT and M.PAGAT (Au and Ag doped) 0.1 mM, 1 mM, 10 mM and 100 mM. Upon the continuous photon energy range, the absorption processes, namely photoelectric absorption and pair production lead to complete removal of photons, so the lifetime of photons in the material is small. Hence, they do not exist for a longer period of time, resulting in less buildup factor at lower and higher energy regions. In the case of the scattering processes i.e. Compton scattering, the photons are not completely removed but their energies are only degraded, resulting in the accumulation of photons. They exist for a long time in the material, thus this process results with more multiple scattered photons increasing buildup factor in the medium. A sharp peak in EABF values was observed at 80 keV energy as shown in Fig. 6 (d and e) which may be due to K-absorption edge of Au at around 80 keV.

Around the K-edge of high Z elements, mass attenuation coefficients jumps into a huge value in the upper side of the K-edge and the element has two mass attenuation coefficients corresponding to the lower and upper side of the edge.

This abrupt change in mass attenuation coefficient could lead a sharp peak in buildup factor. Then the EABF values increase with

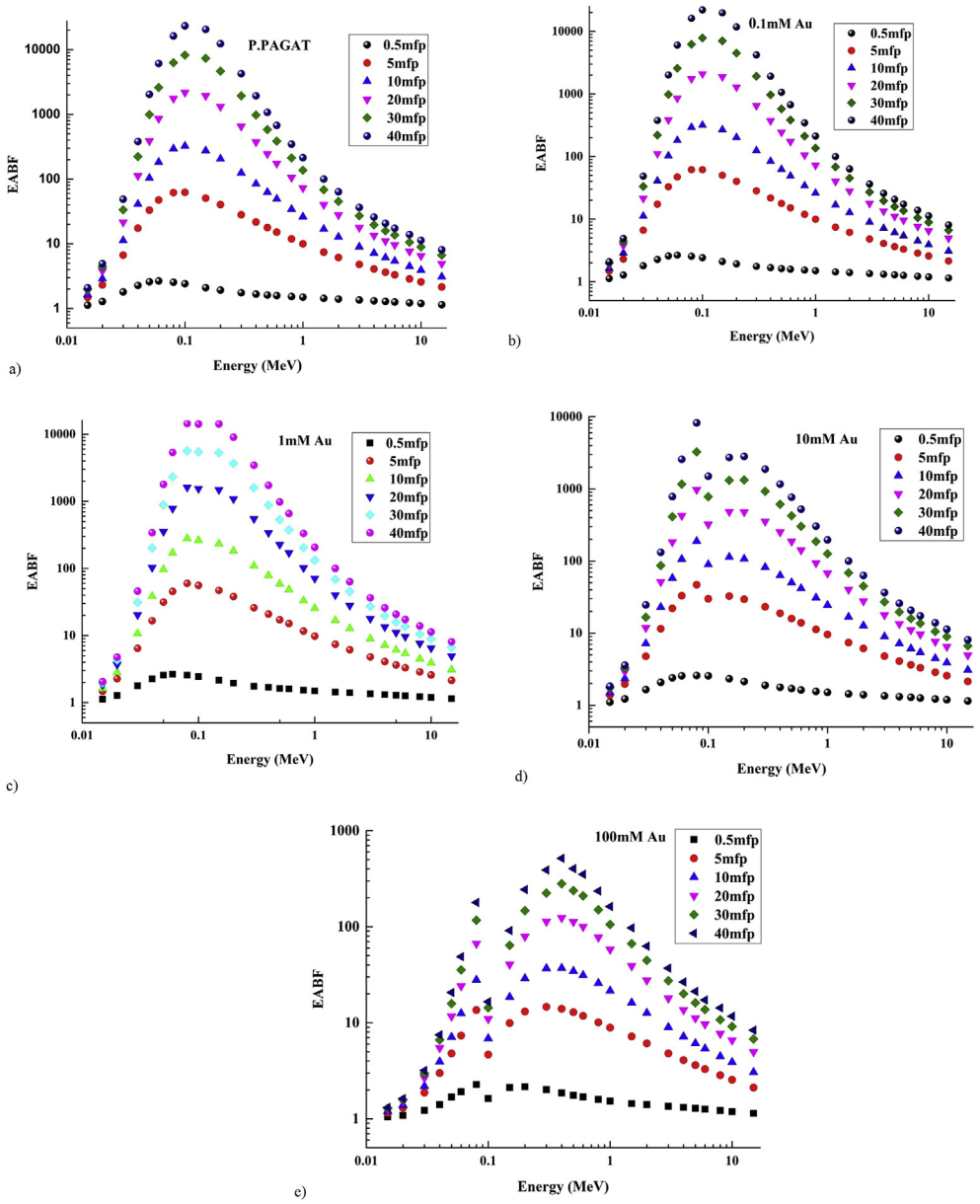

Fig. 7. Variation of the energy absorption buildup factor with photon energy for selected penetration depths up to 40 mfp for the Au doped gels: a) P.PAGAT (0 Mm), b)0.1 mM, c) 1 mM, d)10 mM, e)100 mM.

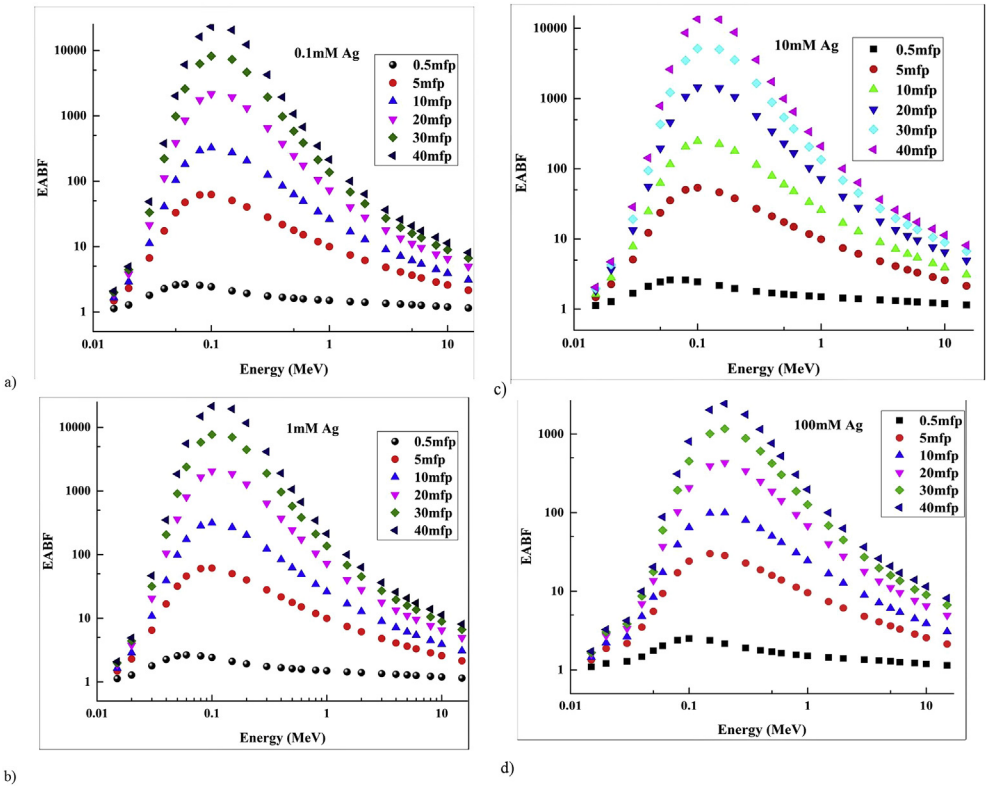

Fig. 8. Variation of the energy absorption buildup factor with photon energy for selected penetration depths up to 40 mfp for the Ag doped gels: a) 0.1 mM, b) 1 mM, c)10 mM, d) 100 mM.

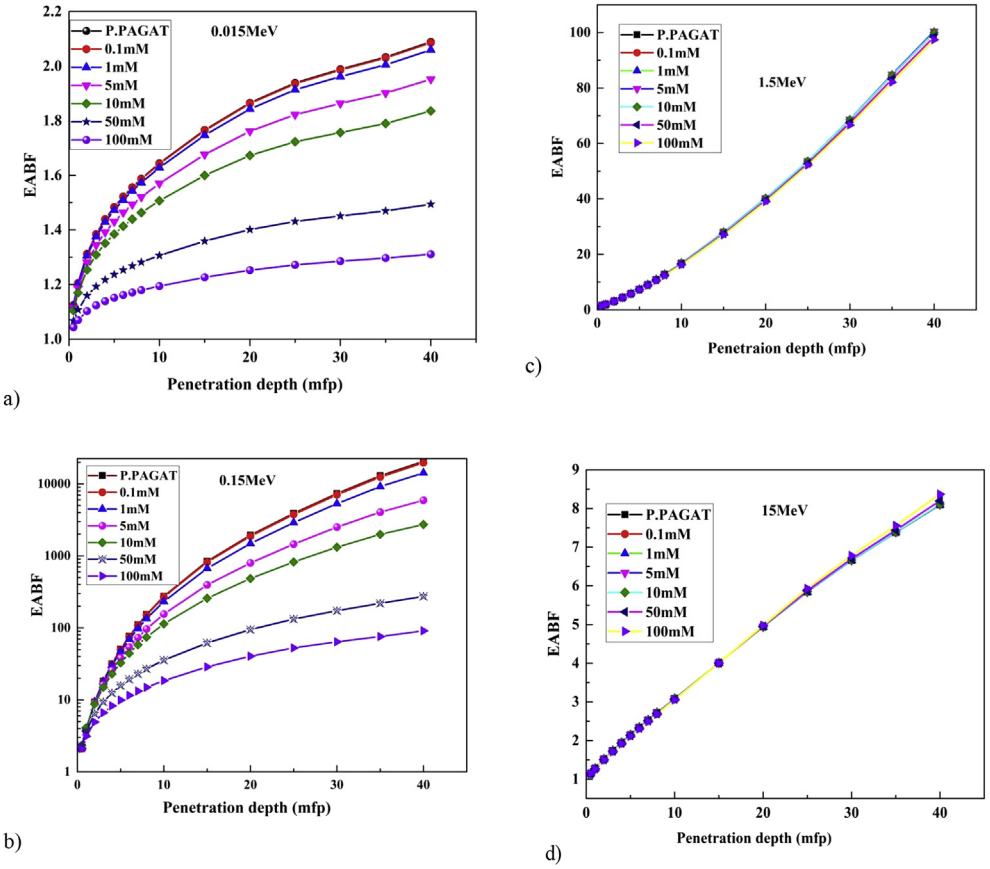

Fig. 9. (a–d). EABF vs penetration depth of different concentration of Au doped MPAGAT for selected Energy (0.015, 0.15, 1.5 and 15 MeV).

the increase in photon energy and show maximum at 0.1 MeV due to predominance of Compton scattering in the intermediate-energies. In Compton scattering photons are not completely removed but just degraded in energy. Finally, BF values start decreasing with the further increase in photon energy due to pair production. We found that EABF values were increasing for all gel dosimeters with increasing penetration depths which might be due to the increase in multiple scattering as the penetration depth increases.

3.5. Variation of energy absorption buildup factor with penetration depth and chemical composition for Au and Ag doped MPGAT

From Figs. 9 and 10, it is clearly seen that, for energy 0.015 and 0.15 MeV the EABFs were increased when penetration depth increased, but for energy 1.5 and 15 MeV the increasing pattern was still remaining at the same time but BF does not change much with chemical composition of the gel materials. EABFs for 0.015 and 0.15 MeV increased with decrease in concentration of Au. In these energies the variation in EABFs between PAGAT and 0.1 mM doped MPAGAT were negligible. The maximum EABF was found as 20557.4 at 0.15Mev for PAGAT while for 0.1 mM of Au doped MPAGAT it was 19659.4 at 0.15 MeV. Minimum EABF was found as 1.044 at 0.015 MeV for 100 mM doped MPAGAT. The discrepancy in EABF for PAGAT and Au doped MPAGAT (for 0.1, 1, 5, 10, 50 and 100 Mm concentration) is very less and constant. At the energy 0.015 and 0.15 MeV maximum number of photon absorbed by photo electric absorption process for Au doped M.PAGAT, this absorption was higher in higher concentration. So, multiple scattering was less in Au doped M.PAGAT and it was very less for higher concentration, this could lead to reduction in the EABF for Au doped MPGAT gel. The same argument holds for Ag doped MPGAT. The maximum EABF for Ag doped MPAGAT was 20441.18 at 0.15 MeV for 0.1 mM concentration. It was higher than Au doped MPGAT for the same energy and same concentration. Since, Ag has less atomic number than Au the photoelectric absorption cross section was less in Ag doped M.PAGAT and the complete absorption of photons is less, thus it leads a relative increase in the Compton interaction when compared to Au doped one. This increases the EABF more in Ag doped M.PGAT than Au doped M.PGAT. Since P.PAGAT was slightly modified by adding Au and Ag, the chemical composition of the M.PAGAT does not make any impact on EABF. At energy 1.5 MeV (Figs. 8 (c) & 9 (c)), where only Compton scattering is the dominant interaction process it leads an increase in EABF and it seems to be independent of chemical composition. The same explanation can be true at energy 15 MeV(Figs. 8 (d) & 9 (d)), where only pair production is the dominant interaction process and the multiple scattering was less, this leads to reduction in the EABF and seems to be independent of chemical composition as well.

3.6. Variation of exposure buildup factor with energy and penetration depth for MPGAT

Figs. 11 and 13 show the variation of the EBF (for Au and Ag doped PAGAT gel) as a function of energy. Variation in EBF seems to be similar to the variation in EABF. Since the EBF is based on the energy absorption response of air while EABF refers to that absorbed or deposited energy in the attenuating material, there are significant differences between EABF and EBFin the continuous energy region [12]. A sharp peak in EBF values was observed at 80 keV as shown in Fig. 11(c) which may be due to K-absorption edge of Au at around 80 keV. Figs. 12 and 14 show the variation of

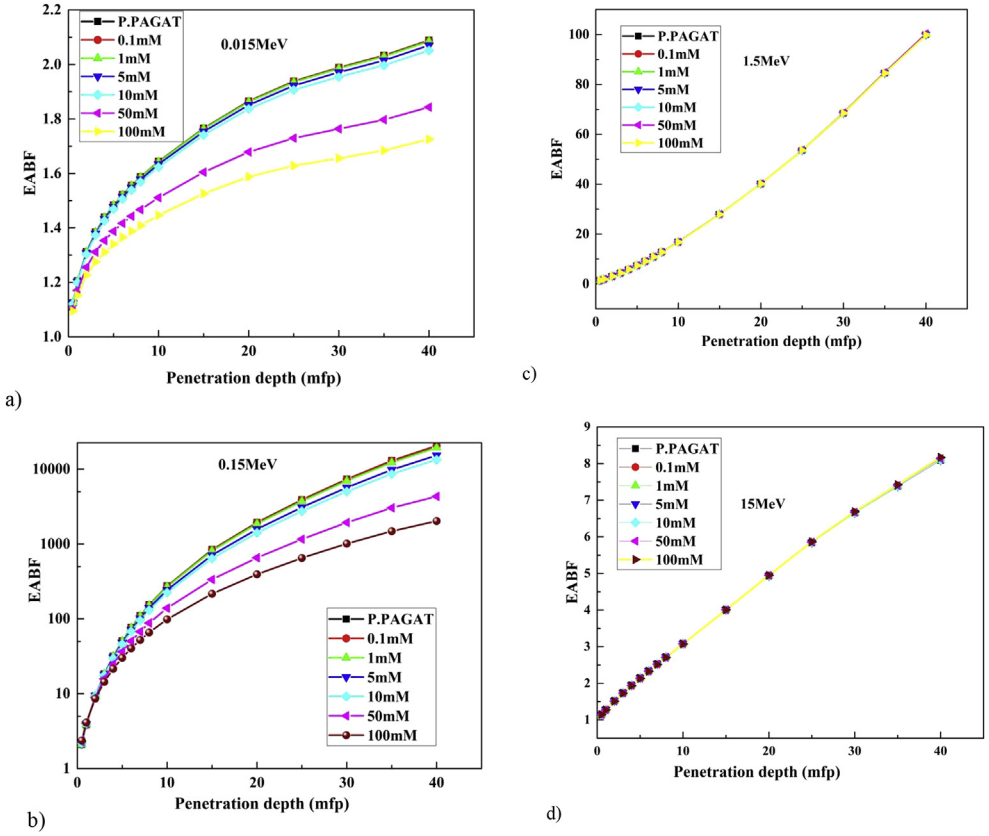

Fig. 10. (a–d). EABF vs penetration depth of different concentration of Ag doped MPAGAT for selected Energy (0.015, 0.15, 1.5 and 15 MeV).

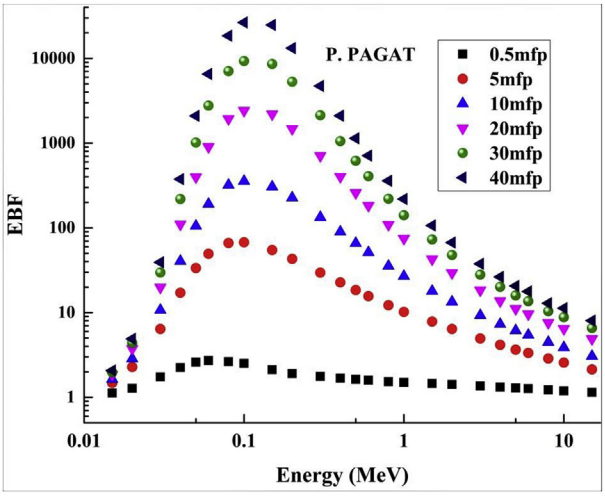

a)

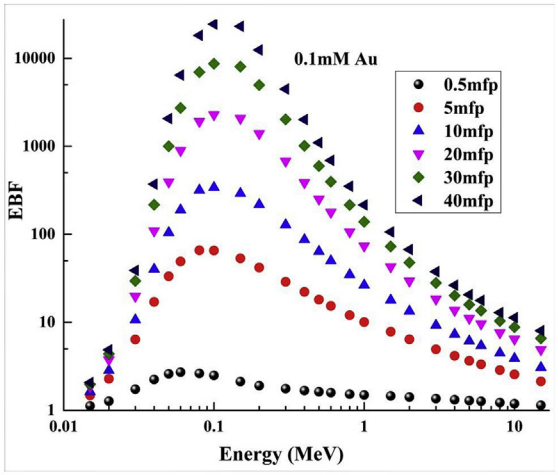

b)

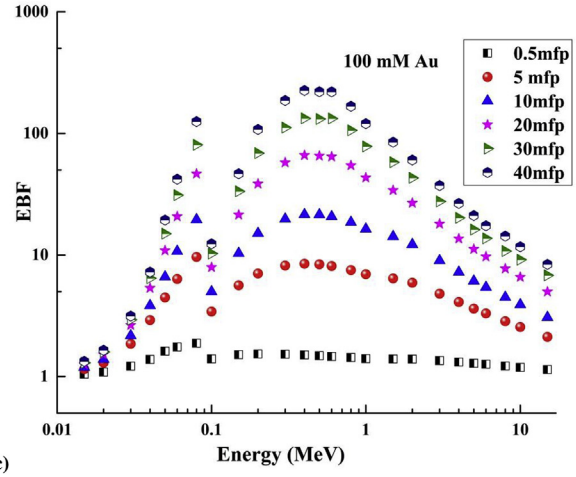

c)

Fig. 11. Variation of the energy absorption buildup factor with photon energy for selected penetration depths up to 40 mfp for the Au doped gels: a) P.PAGAT, b)0.1 mM and c)100 mM.

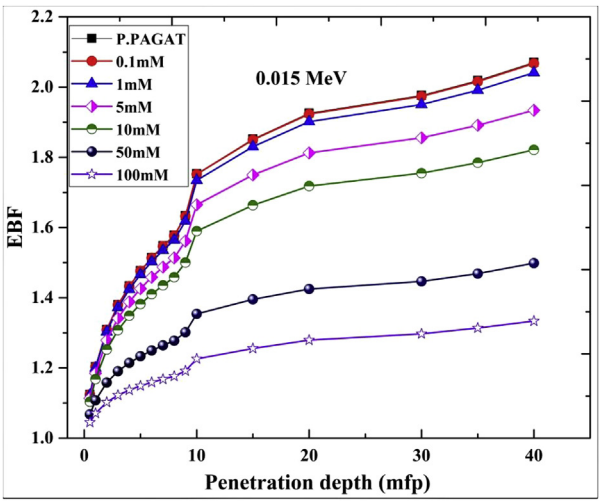

a)

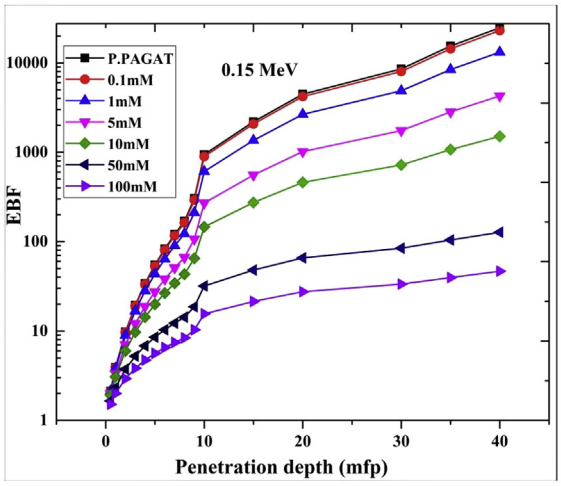

b)

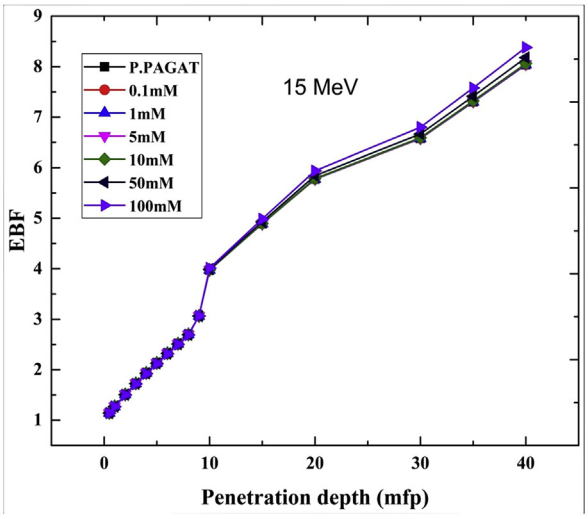

c)

Fig. 12. (a, b and c). EBF vs penetration depth of different concentration of Au doped MPAGAT for selected Energy (0.015, 0.15, and 15 MeV).

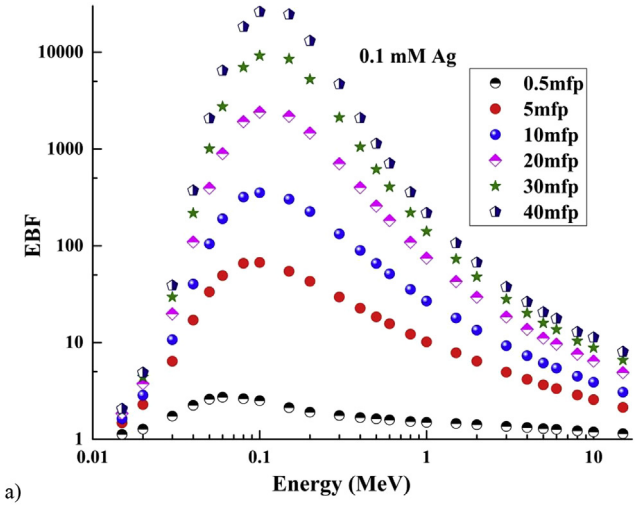

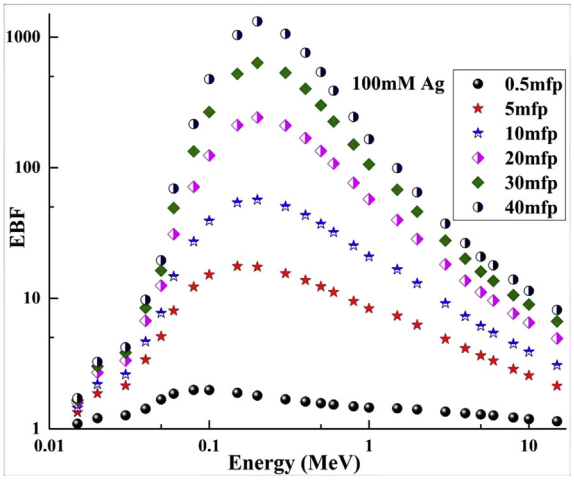

Fig. 13. Variation of the energy absorption buildup factor with photon energy for selected penetration depths up to 40 mfp for the Ag doped gels: a) 0.1 mM and b) 100 mM.

EBF as a function of penetration depth for Au and Ag doped MPAGAT. In intermediate energy region (0.15 MeV) for mfp $\leq$ 20, it was observed that the EABF values are higher than EBF because photons build-up more. Although the EABF and EBF show similar variations as a function of the photon energy, penetration depth and chemical composition, significant differences have been noticed between the EABF and EBF at some photon energies for different concentration of Au and Ag in MPAGAT. The maximum difference between EABF and EBF was noticed at intermediate energy (0.15 MeV) for 100 mM Au doped PAGAT gel. This difference was less at lower concentration of Au in PAGAT gel.

3.7. *Verification of mass attenuation coefficient by Monte Carlo simulation*

Fig. 15 shows the photon histories from source to detector. Mass attenuation coefficients obtained by XCOM [23] database was compared with the Monte Carlo simulation method. Fig. 16 shows the plot between thickness of the gel and log (I/I_0) which was obtained by Monte Carlo results and the slop gives the linear

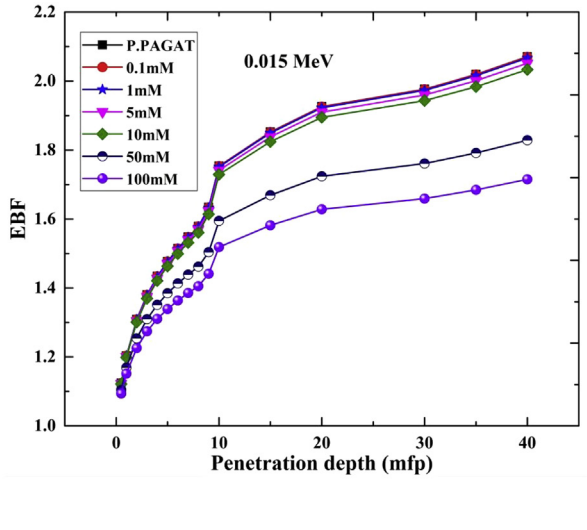

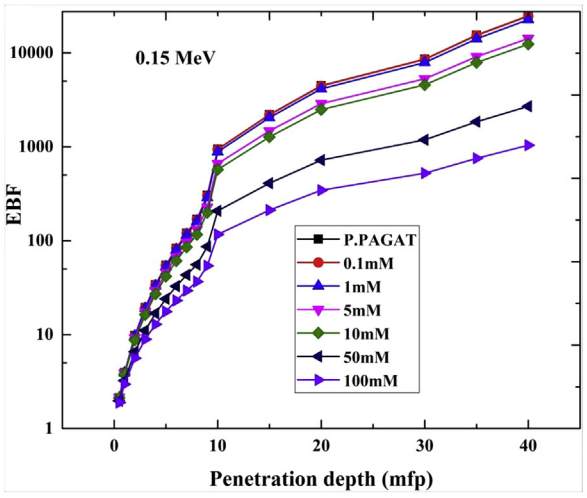

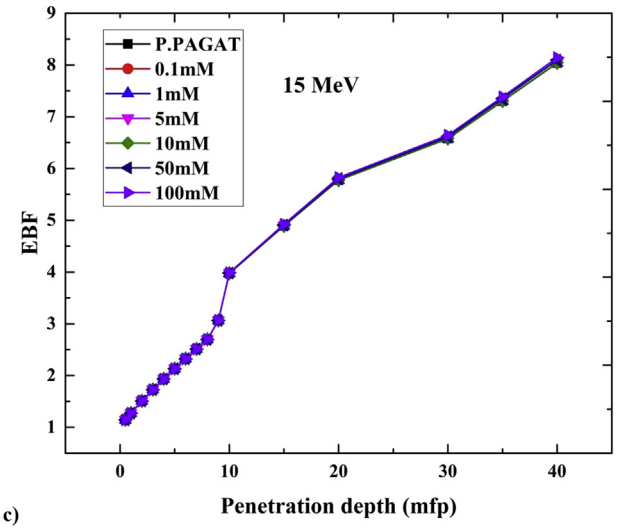

Fig. 14. (a, b and c). EBF vs penetration depth of different concentration of Ag doped MPAGAT for selected Energy (0.015, 0.15, and 15 MeV).

attenuation coefficients, this linear attenuation coefficients were

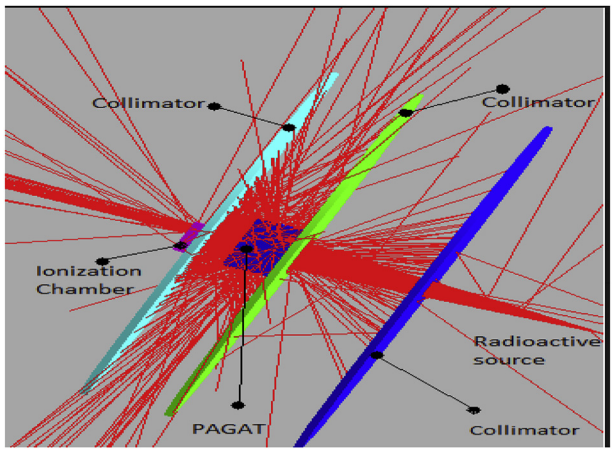

Fig. 15. Histories of photons from source to detector simulated by Monte Carlo simulation.

divided by the density of the gel to obtain mass attenuation coefficient.

The results of XCOM [23] were compared with that of Monte Carlo simulations and a good agreement has been obtained (Table 6).

Table 6
XCOM and Monte Carlo comparison of mass attenuation coefficient.

Gel	XCOM			Monte Carlo		
	0.01 MeV	0.1 MeV	1 MeV	0.01 MeV	0.1 MeV	1 MeV
P.PAGAT	5.141	0.165	0.0704	5.211	0.149	0.0666
Au.PAGAT	5.300	0.166	0.07041	5.252	0.150	0.0669
Ag.PAGAT	5.153	0.165	0.0704	5.228	0.149	0.0667

4. Uncertainties

Hubbell [26] reported that the envelope of the uncertainty of mass attenuation coefficient is in the order of 1–2% in the energy range from 5 keV to a few MeV. In case of the energies of 1–4 keV, the discrepancies are known to reach to a value of 25–50%.

Chantler [27] has successfully addressed the huge discrepancies in mass attenuation coefficient below 4 keV and derived new theoretical results of substantially higher accuracy in near-edge soft X-ray regions in detail. The most interested energies widely used in biological, medical and shielding applications cover the energies larger than 5 keV; hence the results for the selected gel dosimeters should have an uncertainty of a few percentages. Mass attenuation coefficients of any compound materials like polymer gel is derived by mixture rule. This mixture rule is not valid for the K-absorption edge of the compound material and the atomic wave function of the material altered by the molecular, chemical and crystalline environment. This environment factors are not accounted by mixture rule [28–30]. But it causes the errors very few percent in the energy range above 10 keV. Since both Z_{eff} and EABF are evaluated above 10 keV in the present study, the expected error is within the limit. On the other hand, it was reported by Taylor et al. (2012) that uncertainties in Z_{eff} estimated by Auto-Zeff program is within 1–2% [19].

The five parameter geometric progression fitting (GP) method was used to evaluate EABF. The absolute value of the maximum deviation of exposure buildup factors for water in the GP fitting is within 0.5–3% [31], in the three-exponential approach is within 0.4–9.3%, in the Berger approach is within 0.9–42.7% and in the Taylor approximation is within 0.4–53.2% [32]. GP fitting method showed less discrepancy than other methods and therefore it was adopted for calculation of EABF in the present study.

5. Conclusion

While any high Z material added in the well-known concentration of polymer gel like PAGAT may provide advantage of dose enhancement, the doped gel must be as much water equivalent as at the same time. In the present study, the water equivalency of metal doped PAGAT was analyzed successfully for different concentration of Au and Ag in terms of Z_{eff}. Due to higher mole fraction of Au and Ag in the MPAGAT gel, Z_{eff} calculated by the Mayneourd's formula is not in agreement with that calculated by interpolation method. In the interpolation method, both materials, when added with metals obviously affected the water equivalency of the PAGAT. Surprisingly, M.PAGAT doped with less concentration of Au and Ag showed better water equivalency than P.PAGAT gel. It was obtained that PAGAT doped in higher concentration of Au and Ag (50 and 100 mM) cannot be considered as water equivalent gel. Below 0.2 MeV, MPAGAT doped in 5 and 10 mM concentrations can be accepted as water equivalent gel. From 0.01 to 1 mM, MPAGAT can be accepted as water equivalent gel from 10 keV to 1 GeV. Although the lower concentration showed less discrepancy in Z_{eff} relative to

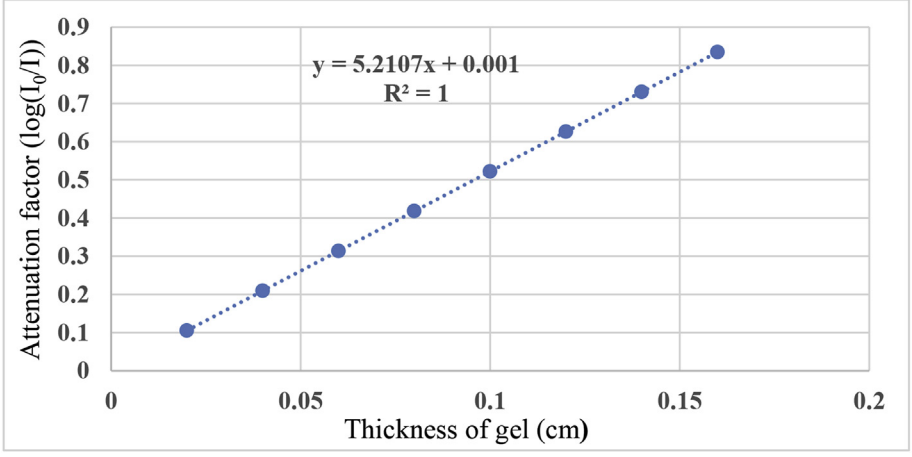

Fig. 16. Intensity of the photon beam passed through PAGAT gel simulated by Monte Carlo simulation.

water, special care must be taken for K-edges of the material due to drastic changes in Z_{eff}. In addition to Z_{eff}, another important parameter EABF was also investigated for P.PAGAT and M.PAGAT from 0.015 to 15 MeV up to 40mfp. Significant variation in EABF has been noticed for P.PAGAT and M.PAGAT in the intermediate energy region where Compton scattering is the dominant interaction process. At 1.5 and 15 MeV, the variation of EABF with different penetration depth appears to be almost independent of the chemical composition of the gel. XCOM results of mass attenuation coefficient were successfully compared with Monte Carlo simulated results and their reliability was excellent. Since the high Z materials were added in the gel, more research is substantially required to support this preliminary investigation.

Acknowledgement

The authors thank Dr. William de Souza Santos, (INFIS/UFU) Uberlandia, MG, Brazil for technical support in the Monte Carlo simulation.

References

[1] Geoffrey S. Ibbott, J. Phys. Conf. Ser. 3 (2004) 58–77 (IOP Publishing).
[2] P. Sellakumar, E.J.J. Samuel, S.S. Supe, Rep. Pract. Oncol. Radiother. 11 (2006) 247–251.
[3] J.P. Fernandes, B.F. Pastorello, D.B. de Araujo, O. Baffa, Phy.Med. Biol. 53 (2008) N53.
[4] A. Hiroki, S. Yamashita, M. Taguchi, J. Phys. Conf. Ser. 573 (2015) 012028 (IOP Publishing).
[5] N.R. Kakade, S.D. Sharma, J. Cancer Res. Ther. 11 (1) (2015) 94.
[6] M. Mahdavi, M. KhademAbolfazli, S.R.M. Mahdavi, G. Ataei, J. Biomed. Phys. Eng. 3 (2013) 37.
[7] M. Kurudirek, Radiat. Phys. Chem. 102 (2014) 139–146.
[8] S.R. Manohara, S.M. Hanagodimath, L. Gerward, Phy. Med. Biol. 53 (2008) N377.
[9] S.R. Manohara, S.M. Hanagodimath, L. Gerward, Med. Phy. 36 (2009) 137–141.
[10] S.R. Manohara, S.M. Hanagodimath, L. Gerward, Radiat. Phys. Chem. 79 (2010) 575–582.
[11] S. Gupta, G.S. Sidhu, Int. J. Sci. Res. Publ. 2 (2012) 1–7.
[12] M. Kurudirek, Y. Özdemir, J. Radiol. Prot. 3 (2011) 117.
[13] M.I. Sayyed, S.I. Quashu, Z.Y. Khattari, J. Alloys Compd (2016), http://dx.doi.org/10.1016/j.jallcom.2016.11.160.
[14] Shams Issa, Mohamad Sayyed, Murat Kurudirek, J. Phys. Sci. 27 (2016) 97–119.
[15] Shams A.M. Issa, A.M.A. Mostafa, J. Alloys Compd. 695 (2017) 302–310.
[16] A.J. Venning, K.N. Nitschke, P.J. Keall, C. Baldock, Med. Phys. 32 (2005) 1047–1053.
[17] S. Brown, A. Venning, Y. De Deene, P. Vial, L. Oliver, J. Adamovics, C. Baldock, Appl. Radiat. Isot. 66 (2008) 1970–1974.
[18] T. Gorjiara, R. Hill, Z. Kuncic, S. Bosi, J.B. Davies, C. Baldock, Phys. Med.Biol. 56 (2011) 4685–4699.
[19] F.M. Khan, The Physics of Radiation Therapy, Williams and Wilkins publishers, Maryland, USA, 1994.
[20] M.L. Taylor, R.L. Smith, F. Dossing, R.D. Franich, Med. Phy. 39 (2012) 1769–1778.
[21] Danial Salehi, Dariush Sardari, M.S. Jozani, Adv. Mater. Res. 4 (2015) 23–30.
[22] American National Standard for Gamma-Ray Attenuation Coefficients and Buildup Factors for Engineering Material, 1991. ANSI/ANS-6.4.3.
[23] M.J. Berger, J.H. Hubbell, S.M. Seltzer, J. Chang, J.S. Coursey, R. Sukumar, D.S. Zucker, K. Olsen, XCOM: Photon Cross Section Database (version 1.5) [Online] Available: http://physics.nist.gov/xcom, 2010 [Tuesday, 06-Jun-2017 03:56:28 EDT]. National Institute of Standards and Technology, Gaithersburg, MD. Originally published as Berger, M.J. and Hubbell, J.H., "XCOM: Photon Cross Sections on a Personal Computer," NBSIR 87-3597, National Bureau of Standards (former name of NIST), Gaithersburg, MD (1987); and as Berger, M.J. and Hubbell, J.H., "NIST X-ray and Gamma-ray Attenuation Coefficients and Cross Sections Database," NIST Standard Reference Database 8, Version 2.0, National Institute of Standards and Technology, Gaithersburg, MD (1990).
[24] M.J. Maron, Numerical Analysis: a Practical Approach Macmillan, NY, 1987.
[25] J.K. Shultis, R.E. Faw, "An MCNP primer", Kansas State University, Manhattan, 2011.
[26] J.H. Hubbell, Phy. Med. Biol. 44.1 (1999) p. R1.
[27] C.T. Chantler, J. Phys. Chem. Ref. Data. 29.4 (2000) 597–1056.
[28] P. Vishwanath Singh, N.M. Badiger, J. Med. Phy 39 (2014) 24–31.
[29] B.R. Kerur, S.R. Thontadarya, B. Hanumaiah, X-Ray Spectrom. 22 (1993) 13–16.
[30] U. Turgut, O. Simsek, E. Buyukkasap, PRAMANA. 69 (2007) 199–207.
[31] Y. Harima, Y. Sakamoto, S. Tanaka, M. Kawai, Nucl. Sci. Eng. 94 (1986) 24–35.
[32] Y. Harima, Y. Sakamoto, S. Tanaka, M. Kawai, T. Fujita, T. Ishikawa, M. Kinno, K. Hayashi, Y. Matsumoto, T. Nishimura, Applicability of Geometrical Progression Approximation (GP Method) of Gamma-ray Buildup Factors, Japan Atomic Energy Research Institute, 1986 (JAERI)-M 86–071.